

## A study of EAS muon near core of showers of size $10^{4.3}$ to $10^{6.3}$

S. K. Sarkar<sup>a</sup>, K. Ghosh<sup>a</sup> and R. K. Chhetri<sup>b</sup>

(a) High Energy & Cosmic Ray Research Centre, North Bengal University, Darjeeling 734430, India

(b) Sikkim Govt. College, Gangtok 737102, India

Presenter: K. Ghosh (kasturighosh@rediffmail.com), ind-ghosh-Kasturi-abs1-he12-oral

The distribution of muons near core of showers of size  $10^{4.3}$ - $10^{6.3}$  particles is studied by measuring the density of muons with different energies by NBU air shower array spread over an area of  $\sim 3000$  m<sup>2</sup> at sea level. The measured muon lateral distribution (MLD) with different energy threshold and muon energy spectrum show significant consistency when compared with measurements of various other groups. The numbers of muons ( $N_{\mu}^{tr}$ ) in EAS of different sizes are estimated from measured MLD up to a distance of 35m and their variation with shower size is studied. The present study of muon abundance, in different shower sizes, indicates the position of knee in the primary spectrum and possible change of primary composition.

### 1. Introduction

Among the different components of EAS, knowledge of radial distribution together with energy distribution of muons in EAS is regarded of prime importance as it is expected to be sensitive to both the primary composition and characteristics of particle interaction at high energies. Many simulations of cosmic ray EAS have strongly indicated that various measurable properties of muons in EAS like lateral density distribution, integrated energy spectrum, the muon to electron ratio in given size of the EAS etc. could be potential mass sensitive parameters. The experimental study carried out with NBU EAS array (described in brief in the next section and in detail in our previous publications [1]), is intended to study different properties of muons associated with EAS of size range  $\sim 10^4$  to  $10^6$  particles. Our preliminary measurements reported in previous publications, which is seen to be consistent with measurements of other experiments, have been used by different investigators[2] to compare with their theoretically simulated results. In this paper, we are reporting our measurements carried out when a major change/addition was made in the array. These results with improved statistics, is hoped to provide a firmer base for comparing with the theoretical predictions for different primary composition. Furthermore, the EAS of sizes measured by NBU EAS array is estimated to be initiated by primaries having energy  $\sim 10^{15}$  to  $10^{16}$  eV and this is the region of primary spectrum where the so called knee is observed. The explanation of the existence of such a feature in primary spectrum and their possible reflection in the properties of different EAS components have been of great interest in contemporary EAS studies. Our measurements of muon component of EAS also have shown some indication of change in primary composition, which is presented in the result section.

### 2. Experimental setup & Data analysis

The NBU EAS array; initially started in 1980 with 16 plastic scintillation counters, two shielded muon magnet spectrograph and one neon flash tube chamber spread over an area of 800 m<sup>2</sup> at near sea level (130m. a.s.l.), has grown over the years. The addition of 8 fast timing scintillation detectors in 1994 has provided the array with the facility of ascertaining the arrival direction of the shower. Further in 1998 few more detectors were added and all the data recording system was computerised. At the time of experiment whose results are being reported in this paper, 35 plastic scintillation detectors spread over an area of  $\sim 3000$  sq. meter were used. The plastic scintillation counters, used to measure the electron density at different points of the incident EAS front, are each of the size 0.25 m<sup>2</sup> and have a thickness of 5cm. The two shielded muon magnet spectrographs of each with area of 1m<sup>2</sup> and of maximum detectable momentum  $\sim 500$  GeV/c, has two wings. The concrete shielding provided by the housing of the spectrographs along with additional lead and concrete absorbers

placed above each wing gives lower cutoff muon energy of 2.5 GeV detectable by the spectrograph. The muon energy is estimated by the deviation observed in the muon trajectory which is recorded by four neon flash tube hodoscopes with an accuracy of 1.4 GeV at  $E_\mu=20$  GeV. The condition for triggering and hence subsequent recording of the shower incident on the array is such that, a shower is recorded only if the registered density in four central triggering detectors are  $\geq 4$  particles/m<sup>2</sup> or if the observed particle density in any three of the four central detectors and in any one of the four triggering detectors situated at the four corners of the array are  $\geq 4$  particles/m<sup>2</sup>. The basic parameters of each of the incident showers, viz. core position ( $X_0, Y_0$ ), shower age(s) and shower size ( $N_e$ ) are determined by fitting the measured electron density at different points of shower front to NKG function. The uncertainties in determining these parameters for the new extended setup, estimated by the same method of artificial shower analysis as reported in our earlier paper[3], is seen to be  $\pm 2$ m (core position),  $\pm 0.09$ (s) and  $9.7\%$ ( $N_e$ ) at typical shower size of  $5 \times 10^5$  particles. The uncertainty in estimating the arrival direction is estimated to be  $1.6^\circ$  at  $60^\circ$  zenith. Observed showers were grouped according to their size in seven different size bins in the range  $10^{4.3}$  to  $10^{6.3}$  particles. And, the average muon density in a shower as a function of the radial distance from the shower core was estimated for each of various size bins using the average density defined as,  $\rho_\mu(\geq E_\mu, N_e, r) = N(\geq E_\mu, N_e, r)/(N_t(N_e, r) * A)$

where  $N$  is the total number of muons recorded in a particular distance bin with average value  $r$  for a particular size bin with average size  $N_e$  and having energy  $\geq E_\mu$ ,  $N_t$  is the total number of the showers having size in the same bin and recorded during the same time interval.  $A$  is the effective area of the muon detectors.

### 3. Experimental results

#### 3.1 Muon lateral distribution

Some representative measured muon lateral distribution with energy  $E_\mu \geq 2.5, 10, 25$  and  $100$  GeV are shown in fig.1 along with the measurements of other experiments like MSU[4], KASCADE[5], Lodz and KIEL[6 and reference therein], GAMMA[7]. Our measurements, within statistical error indicated in the figure, are seen to be consistent with other groups. Furthermore, the measured distribution is fitted, shown by the solid curves in the figure, with a parameterization of the form,

$$\rho_\mu(\geq E_\mu, N_e, r) = A * r^{-\alpha(\geq E_\mu, N_e)} * \text{Exp}(-r/r_0) \quad (1)$$

where  $r_0$  is a simple logarithm function of shower size which decreases with it, and the power exponent  $\alpha(\geq E_\mu)$  is seen to increase uniformly with muon threshold energy but is seen to remain almost constant within statistical error upto average shower size  $5.5 \times 10^5$  particles with significant increase in higher sizes. The variation of exponent  $\alpha(\geq E_\mu)$  with shower size for muon threshold energy of  $E_\mu \geq 2.5$  GeV are shown in fig. 2.

#### 3.2 Muon Energy spectrum

Some of the measured energy spectrum of muons in EAS of sizes  $2.5 \times 10^5$  and  $1.1 \times 10^6$  at distance 20-30m from shower core are shown in fig. 3 along with some representative measurements of MSU experiment [8] and are seen to be consistent with them. The measured energy spectrum is also fitted with an equation of the form,

$$\rho_\mu(\geq E_\mu, N_e, r) = K * ((E_\mu + 2)/4.5)^{-\lambda} e^{(-\eta * E_\mu)} \quad (2)$$

The best-fitted lines are shown in the figure as solid curves and the values of parameter  $\lambda$  is presented in table-1 whereas the value of  $\eta$  is nearly constant ( $0.008 \pm 0.001$ ) for the measured shower size range.

#### 3.3 Muon-to-electron ratio

The total number of muons ( $N_\mu$ ) contained in a given shower size range can be estimated by integrating equation (1) for all possible values of distance ( $r$ ) extending upto infinity. However, since the distribution is

**Table 1.** The fitted values of  $\lambda$  for the core distance (20-30)m

$N_e$	$3.3 \times 10^4$	$6.4 \times 10^4$	$1.4 \times 10^5$	$2.5 \times 10^5$	$5.5 \times 10^5$	$1.1 \times 10^6$	$1.7 \times 10^6$
$\lambda$	$0.30 \pm 0.03$	$0.29 \pm 0.04$	$0.40 \pm 0.04$	$0.40 \pm 0.04$	$0.37 \pm 0.05$	$0.29 \pm 0.03$	$0.27 \pm 0.04$

only measured upto certain limited distance, many authors have pointed out that such integration would lead to overestimation of muon number and hence, have suggested integrating the equation representing the lateral distribution of muons (LDF) upto limited distance of detection, yielding the so called truncated number of muons ( $N_\mu^{tr}$ ). As such, in our analysis too, the ( $N_\mu^{tr}$ ) have been calculated by integrating equation (1) within a distance of 4-35m. The detection efficiency of our array is seen to be more than 95% within a distance of 35m from centre of the array, beyond which it falls rapidly. We also wanted to use only those showers, whose core falls well within the array, and hence the choice of distance range upto 35m. The observed variation of truncated muon number ( $N_\mu^{tr}$ ) with shower size  $N_e$  for different muon energy threshold ( $\geq E_\mu$ ) are shown in fig.4. The variation is seen to be uniform till the range of shower size with average value  $5.5 \times 10^5$  beyond which the muon content increases significantly in the higher size range. As a result, it is observed that the variation within the studied shower size range could not be fitted with a single power exponent. The exponent of power fit of the form ( $N_\mu^{tr} \propto N_e^\delta$ ) in two ranges of shower sizes  $\delta_1$  &  $\delta_2$  below & above  $5.5 \times 10^5$  respectively are shown in table-2.

**Table 2.** The fitted values of  $\delta_1$  &  $\delta_2$ 

$\geq E_\mu$ (GeV)	2.5	5.0	10.0
$\delta_1$	$0.67 \pm 0.02$	$0.64 \pm 0.03$	$0.63 \pm 0.02$
$\delta_2$	$0.82 \pm 0.02$	$0.89 \pm 0.04$	$0.96 \pm 0.08$

#### 4. Discussion and conclusion

In the present experimental measurement representing radial and energy distribution of muons in EAS of size  $10^{4.3}$  to  $10^{6.3}$  both the distributions are seen to remain unchanged with shower size up to certain range of shower size with average value  $5.5 \times 10^5$ , beyond which they become significantly steeper. Similar observations have been reported by other groups [9] who have studied lateral distribution of muons at sea level. This steepening of muon distribution in the neighborhood of average shower size  $5.5 \times 10^5$  could be an indication of primary change. And, the shower size of EAS observed at sea level at which such a change is observed corresponds to the primary energy where the so called "knee" is observed. The same kind of feature is also reflected in the measured variation of truncated muon number  $N_\mu^{tr}$  with shower size  $N_e$  for different muon energy threshold ( $\geq E_\mu$ ). A significant difference in slope representing such variation above and below certain value of shower size ( $\sim 5.5 \times 10^5$ ) is seen from table-2. The difference is observed to become more prominent with the increase of muon threshold energy. The theoretical studies of simulating EAS have shown that muon content of EAS induced by heavy primary are much higher than those of proton induced showers. So, our observation of comparatively slower increase of muon content of EAS below size range with average size  $5.5 \times 10^5$  could possibly indicate that the composition below and around knee position is lighter with a hint of changing to heavy beyond the knee of primary.

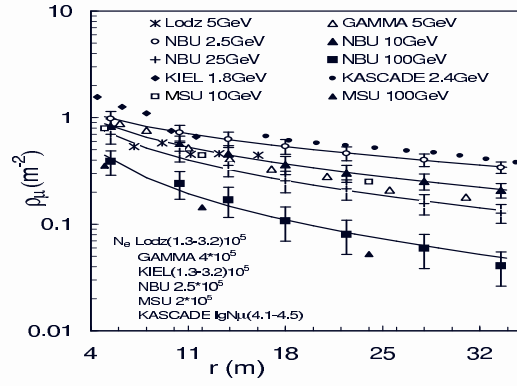


Fig. 1 Lateral distribution of muon

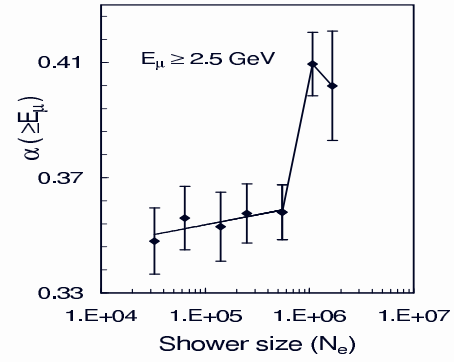
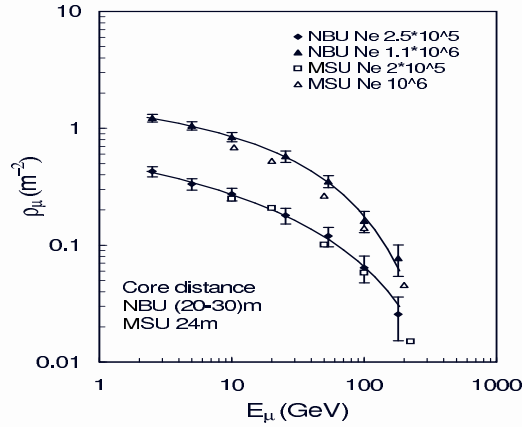
Fig.2 Variation of  $\alpha(\geq E_\mu)$  with  $N_e$ 

Fig.3 Muon energy spectrum

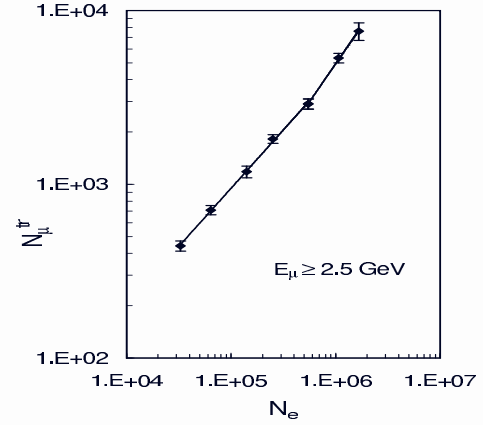


Fig.4 Variation of muon to electron number

## References

- [1] D.K. Basak et al., Nucl. Inst. & Meth. 227, 167 (1984).  
A. Bhadra et al., Nucl. Inst. & Meth. A 414, 233 (1998).
- [2] P.R. Blake et al., J. Phys. G: Nucl. Part. Phys. 24, 217 (1998).  
M.D. Rodriguez-Frias et al., J. Phys. G: Nucl. Part. Phys., 21, 1121 (1995).
- [3] G. Saha et al., Il Nuovo Cimento, 21C, 215 (1998).
- [4] N.V. Grishina et al., 17th ICRC, Paris (1981) 6, 3.
- [5] T. Antoni et al., Astro. Part. Phys., 14, 245 (2001).
- [6] J. Kempa and M. Samorski, 26th ICRC, Utah (1999) 1, 282.
- [7] A.A. Chilingarian et al., ANI workshop, 1998.
- [8] V.B. Atrashkevich et al, 18th ICRC, Bangalore (1983) 11, 229.  
N.V. Grishina et al., 17th ICRC, Paris (1981) 6, 3.
- [9] A. Hungs et al., KASCADE collaboration, Report FZKA6263, (1999).  
V.V. Vashkevich et al., Sov. J. Phys., 47(4), 672 (1988).